



Universiteit  
Leiden  
The Netherlands

## Unraveling the impact of sialic acids on the immune landscape and immunotherapy efficacy in pancreatic cancer

Boelaars, K.; Goossens-Kruijssen, L.; Wang, D.; Winde, C.M. de; Rodriguez, E.; Lindijer, D.; ... ; Kooyk, Y. van

### Citation

Boelaars, K., Goossens-Kruijssen, L., Wang, D., Winde, C. M. de, Rodriguez, E., Lindijer, D., ... Kooyk, Y. van. (2023). Unraveling the impact of sialic acids on the immune landscape and immunotherapy efficacy in pancreatic cancer. *Journal For Immunotherapy Of Cancer*, 11(11). doi:10.1136/jitc-2023-007805

Version: Publisher's Version

License: [Creative Commons CC BY-NC 4.0 license](#)

Downloaded from: <https://hdl.handle.net/1887/3761765>

**Note:** To cite this publication please use the final published version (if applicable).

# Unraveling the impact of sialic acids on the immune landscape and immunotherapy efficacy in pancreatic cancer

Kelly Boelaars <sup>1</sup>, Laura Goossens-Kruijssen,<sup>1</sup> Di Wang,<sup>2</sup> Charlotte M de Winde,<sup>1</sup> Ernesto Rodriguez <sup>1</sup>, Dimitri Lindijer,<sup>1</sup> Babet Springer,<sup>1</sup> Irene van der Haar Àvila,<sup>1</sup> Aram de Haas,<sup>1</sup> Laetitia Wehry,<sup>1</sup> Louis Boon,<sup>3</sup> Reina E Mebius,<sup>1</sup> Nadine van Montfoort <sup>4</sup>, Manfred Wuhrer,<sup>2</sup> Joke M M den Haan,<sup>1</sup> Sandra J van Vliet,<sup>1</sup> Yvette van Kooyk <sup>1</sup>

**To cite:** Boelaars K, Goossens-Kruijssen L, Wang D, *et al.* Unraveling the impact of sialic acids on the immune landscape and immunotherapy efficacy in pancreatic cancer. *Journal for ImmunoTherapy of Cancer* 2023;**11**:e007805. doi:10.1136/jitc-2023-007805

► Additional supplemental material is published online only. To view, please visit the journal online (<http://dx.doi.org/10.1136/jitc-2023-007805>).

Accepted 17 September 2023



© Author(s) (or their employer(s)) 2023. Re-use permitted under CC BY-NC. No commercial re-use. See rights and permissions. Published by BMJ.

<sup>1</sup>Molecular Cell Biology & Immunology, Amsterdam institute for Infection and Immunity, Cancer Center Amsterdam, Amsterdam UMC Location VUmc, Amsterdam, The Netherlands

<sup>2</sup>Center for Proteomics and Metabolomics, Leiden University Medical Center, Leiden, The Netherlands

<sup>3</sup>JJP Biologics, Warsaw, Poland

<sup>4</sup>Department of Gastroenterology and Hepatology, Leiden University Medical Center, Leiden, The Netherlands

## Correspondence to

Professor Yvette van Kooyk; [y.vankooyk@amsterdamumc.nl](mailto:y.vankooyk@amsterdamumc.nl)

## ABSTRACT

**Background** Pancreatic ductal adenocarcinoma (PDAC) is one of the deadliest cancers. Despite the successful application of immune checkpoint blockade in a range of human cancers, immunotherapy in PDAC remains unsuccessful. PDAC is characterized by a desmoplastic, hypoxic and highly immunosuppressive tumor microenvironment (TME), where T-cell infiltration is often lacking (immune desert), or where T cells are located distant from the tumor islands (immune excluded). Converting the TME to an immune-inflamed state, allowing T-cell infiltration, could increase the success of immunotherapy in PDAC.

**Method** In this study, we use the KPC3 subcutaneous PDAC mouse model to investigate the role of tumor-derived sialic acids in shaping the tumor immune landscape. A sialic acid deficient KPC3 line was generated by genetic knock-out of the CMAS (cytidine monophosphate N-acetylneuraminic acid synthetase) enzyme, a critical enzyme in the synthesis of sialic acid-containing glycans. The effect of sialic acid-deficiency on immunotherapy efficacy was assessed by treatment with anti-programmed cell death protein 1 (PD-1) and agonistic CD40.

**Result** The absence of sialic acids in KPC3 tumors resulted in increased numbers of CD4<sup>+</sup> and CD8<sup>+</sup> T cells in the TME, and reduced frequencies of CD4<sup>+</sup> regulatory T cells (Tregs) within the T-cell population. Importantly, CD8<sup>+</sup> T cells were able to infiltrate the tumor islands in sialic acid-deficient tumors. These favorable alterations in the immune landscape sensitized sialic acid-deficient tumors to immunotherapy, which was ineffective in sialic acid-expressing KPC3 tumors. In addition, high expression of sialylation-related genes in human pancreatic cancer correlated with decreased CD8<sup>+</sup> T-cell infiltration, increased presence of Tregs, and poorer survival probability.

**Conclusion** Our results demonstrate that tumor-derived sialic acids mediate T-cell exclusion within the PDAC TME, thereby impairing immunotherapy efficacy. Targeting sialic acids represents a potential strategy to enhance T-cell infiltration and improve immunotherapy outcomes in PDAC.

## WHAT IS ALREADY KNOWN ON THIS TOPIC

⇒ Aberrant glycosylation, particularly overexpression of sialic acids (a process called sialylation), is a common feature in various cancer types contributing to immune evasion and tumor progression. Preclinical studies in other cancer types have shown that targeting sialic acids can improve survival and synergize with immunotherapy. However, the impact of tumor sialylation in pancreatic ductal adenocarcinoma (PDAC) progression, immune evasion and immunotherapy efficacy in vivo has remained unexplored until now.

## WHAT THIS STUDY ADDS

⇒ Our study provides valuable insights into the influence of tumor sialylation on PDAC progression, immune evasion, and immunotherapy efficacy in an in vivo setting. We show that sialic acids in PDAC promote T-cell exclusion and hamper immunotherapy efficacy in vivo. Furthermore, we show that high expression sialylation-related genes in human PDAC is associated with poorer survival probability, decreased CD8<sup>+</sup>T cell numbers, and increased regulatory T cell frequencies. These results elucidate a novel mechanism underlying T-cell exclusion in the PDAC tumor microenvironment (TME).

## HOW THIS STUDY MIGHT AFFECT RESEARCH, PRACTICE OR POLICY

⇒ By understanding the role of sialic acids in shaping the immune microenvironment and promoting T-cell exclusion, this research opens up new avenues for the development of targeted immunotherapeutic strategies in PDAC. Targeting tumor sialylation presents a promising approach to enhance the efficacy of immunotherapy in PDAC. Additionally, the results suggest that expression levels of sialylation-related genes could serve as potential biomarkers for predicting immune responses and treatment outcomes in PDAC.

## BACKGROUND

Pancreatic ductal adenocarcinoma (PDAC) is one of the most aggressive cancer types, often diagnosed at an advanced stage with limited treatment options, resulting in a 5-year overall survival of only 11%.<sup>1</sup> While immune checkpoint blockade (ICB) has revolutionized cancer therapy in various cancer types, its effectiveness in PDAC remains limited.<sup>2</sup> The limited effectiveness of ICB in PDAC is attributed to the relatively low mutational burden and the complex immunosuppressive tumor microenvironment (TME).<sup>3</sup> Understanding the underlying mechanisms responsible for the immunosuppressive TME is crucial to overcome the immune inhibition and to develop novel therapeutic strategies that improve the survival of patients with PDAC.

The TME of PDAC is predominantly composed of desmoplastic stroma, which harbors suppressive immune cells like tumor-associated macrophages (TAMs) and regulatory T cells (Tregs), that hinder effective antitumor immune responses.<sup>4</sup> Both TAMs and Tregs dampen antitumor immunity through the production of tolerogenic cytokines and by inhibiting the activation and function of CD8<sup>+</sup> T cells, natural killer (NK) cells and dendritic cells (DCs).<sup>5,6</sup> Consequently, the abundance of Tregs and TAMs is associated with bad prognosis in patients with PDAC.<sup>7–10</sup> The immunosuppressive nature of the TME is further shaped by cancer-associated fibroblasts (CAFs), which generate dense fibrotic stroma acting as a physical barrier that restricts immune cell infiltration.<sup>4,11</sup> Cytotoxic T cells, the crucial players in antitumor immunity and the effectiveness of ICB, are scarce within the PDAC TME.<sup>12</sup> Even in patients with relatively high T cell numbers, T cells are mainly located within the stroma, distant from the tumor islands.<sup>3,13,14</sup> As a result, many patients exhibit an immune desert phenotype characterized by limited T cells or an immune-excluded phenotype where T cells are present but excluded from the tumor beds.<sup>3</sup> Importantly, studies have shown that the amount of CD8<sup>+</sup> T cells and the proximity of T cells to PDAC tumor cells correlates with increased patient survival.<sup>9,14–16</sup> Therefore, reversing the immunological “cold” PDAC microenvironment to an “inflamed” state, allowing CD8<sup>+</sup> T cells to infiltrate, holds potential to improve the effectiveness of ICB in PDAC.

Aberrant glycosylation is a hallmark of cancer.<sup>17–19</sup> Specific alterations in glycan structures contribute to immune evasion.<sup>19,20</sup> Sialic acids, located at the terminal side of glycans, are commonly overexpressed on various glycoproteins, including mucins like MUC1, in different cancer types.<sup>19,21</sup> Sialic acid on these glycan carriers can interact with sialic acid-binding immunoglobulin-like lectin (Siglecs) receptors expressed on innate and adaptive immune cells, modulating immune responses.<sup>22–23</sup> Numerous studies have demonstrated that tumor sialylation inhibits CD8<sup>+</sup> T and NK cell cytotoxicity.<sup>24–30</sup> Furthermore, activation of the sialic acid-Siglec axis on DCs hampers DC maturation and subsequent priming of T cells and promotes Treg induction.<sup>31–33</sup> Additionally, tumor sialylation polarizes TAMs to a more M2-like phenotype

with tumor promoting properties.<sup>34–38</sup> Notably, in mouse models of melanoma, colorectal, and breast cancer, removal or reduction of tumor sialylation has been shown to result in decreased tumor growth and improved survival,<sup>29,34,39,40</sup> which in melanoma is associated with a favorable shift in the CD8<sup>+</sup>/Treg balance.<sup>29,39</sup> Given their immunosuppressive properties, sialic acids are now recognized as a potential target for immunotherapy.<sup>20</sup>

Preclinical studies targeting tumor sialylation through sialic acid mimetics, sialidase-coupled antibodies, or interference with Siglecs have demonstrated improved survival in mouse models and synergistic effects with ICB in melanoma, colorectal, and breast cancer.<sup>34,39–41</sup> While previous research has highlighted the impact of sialylation on tumor progression and immune modulation in other cancer types, its specific implications in PDAC remain largely unexplored. We have previously shown that sialic acids are overexpressed in patients with PDAC and that high expression of sialylation-related genes is associated with shorter survival probability.<sup>42</sup> Additionally, tumor sialylation promoted the differentiation of monocytes to M2-like TAMs *in vitro*.<sup>42</sup> Importantly, the significance of targeting sialic acids in cancer therapy is gaining recognition, as evidenced by the ongoing phase 1 trial (NCT05259696) evaluating the first agent specifically designed to target sialic acids, which has remarkably enrolled several patients with PDAC (website: <https://palleonpharma.com/education-hub>). However, despite these advancements, there is a notable gap in our understanding of the *in vivo* effects of sialic acids on tumor growth, the immune landscape, and immunotherapy response in PDAC.

The aim of this study was to investigate the influence of tumor sialylation on the *in vivo* dynamics of PDAC, including tumor growth, the immune cell landscape of the TME and draining lymph nodes, as well as immunotherapy response. By employing a sialic acid-deficient model, our objective was to unravel the interplay between sialylation and the immune landscape of PDAC, ultimately providing valuable knowledge for the application of sialic acid targeted therapeutic strategies in this challenging disease.

## METHOD

### Cell lines and cell culture

The murine pancreatic cancer cell line KPC3 was obtained from a primary KPC tumor with mutant *p53* and *K-ras*<sup>43</sup> from a female C57BL/6 mouse (RRID:CVCL\_A9ZK).<sup>44</sup> To generate a sialic acid knock-out (KO) line, KPC3 cells were transfected with a Mock CRISPR/Cas9 construct or a CRISPR/Cas9 plasmid including a gRNA for the *Cmas* gene. Detailed procedure can be found in the online supplemental methods.

### Glycan profiling

Measurement of glycosphingolipids, N-glycans and O-glycans was done on 10 million cells per KPC3 cell line

by PGC nano-LC-ESI-MS/MS. Additional details are included in the online supplemental methods.

### Cell titer blue viability assay

The viability of the KPC3 cells was analyzed with CellTiter-Blue Cell Viability assay (Promega) as an indicator of proliferation after 48 hours of culture, and measured on the FLUOstar Galaxy (MTX Lab systems, excitation 560 nm, emission 590 nm).

### Immunohistochemistry and immunofluorescent stainings

Fresh frozen tumor tissues were cryosectioned at 10  $\mu$ m thickness and stored at  $-20$  degrees. Tissue slides were rehydrated and blocked with Carbo-free blocking solution (Vector Labs) before incubation with 2  $\mu$ g/mL pan-Lectenz (Lectenz Bio) pre-complexed with streptavidin-horseradish peroxidase (HRP). After incubation with pan-Lectenz for 2 hours at room temperature, slides were washed and developed with DAB (DAKO). Slides were dehydrated and mounted with Entellan before brightfield imaging on Vectra Polaris (PerkinElmer).

For immunofluorescent staining, slides were fixed with 1% paraformaldehyde after staining with pan-Lectenz pre-complexed with streptavidin AF488. Slides were incubated overnight at 4°C with anti-CD8 AF555 and anti-EPCAM AF647 in the presence of anti-CD16/CD32 for Fc blocking, washed and mounted with Fluoramount-G (Thermo Fisher Scientific) containing DAPI (1:2000; Invitrogen). All slides were imaged by Vectra Polaris (PerkinElmer).

### Flow cytometry

Staining with 2  $\mu$ g/mL pan-Lectenz (Lectenz Bio) was performed in Hanks' Balanced Salt Solution (HBSS) containing magnesium and calcium (Gibco) supplemented with 0.5% fatty-acid free bovine serum albumin (BSA) (Sigma). The pan-Lectenz reagent was pre-incubated with 1  $\mu$ g/mL streptavidin-APC, and incubated with the cells after life dead staining with Fixable Viability Dye eFluor 450 (eBioscience). Other antibody stainings for flow cytometry were done in phosphate-buffered saline (PBS)/1% BSA, after life dead staining with Fixable Viability Dye eFluor 450. Fluorescence intensities were measured using the Fortessa X-20 and analyzed with FlowJo V.10.

### In vivo tumor experiments

For tumor experiments,  $1 \times 10^5$  KPC3 tumor cells were inoculated subcutaneously (s.c.) in the flank of mice under 2–3% isoflurane. Tumor size was measured three times a week and mice were terminated at day 21 for KPC3 wild-type (WT) tumors, and terminated at day 27 for KPC3 Mock or CMAS KO tumors.

In indicated experiments, mice were treated by intraperitoneal (i.p.) injection of 250  $\mu$ g antagonistic programmed cell death protein 1 (PD-1) antibody (clone RMP1–14, in house, endotoxin-free) two times a week and with 40  $\mu$ g agonistic CD40 antibody (clone 1C10) one time per week, starting from day 16 when tumors were at an average size

of approximately 50–100 mm<sup>3</sup>. The mice were sacrificed individually when tumors reached >800 mm<sup>3</sup>, or when tumors showed beginning ulcer formation to prevent severe discomfort of mice. Untreated mice were i.p. injected with PBS. Additional details have been included in the online supplemental methods.

### Tissue processing and immune cell profiling

Tissues were digested and stained with multicolor antibody panels (online supplemental table 1). Samples were acquired on Cytex Aurora and data was unmixed using the SpectroFlo software. The data was analyzed using FlowJo V.10 and Omiq. Detailed description of tissue digestion, antibody staining and immune cell profiling can be found in the online supplemental methods.

### Transcriptomic analysis

The single-cell RNA sequencing data of patients with PDAC published by Peng *et al* was downloaded from the Genome Sequence Archive project PRJCA001063 as preprocessed row data and imported into the package *Seurat* (v3) for downstream analysis as described previously.<sup>42–45</sup> The function *AddModuleScore* was used to generate a gene score for the donor synthesis gene set (*GNE*, *NANS*, *NANP*, *CMAS*, *SLC35A1*). The data analysis on bulk-sequencing data was performed on 150 pancreatic cancer samples from the PanCanAtlas Publications (<https://gdc.cancer.gov/about-data/publications/pancanatlas>) using R V.4.2.2. Samples classified as normal, pseudo-normal, or non-PDAC were excluded from the analysis.<sup>46</sup> Cell types were estimated by bulk RNA-sequencing deconvolution (*Cibersort*) in package *IOBR* V.0.99.9. Enrichment score for the donor synthesis gene set per individual sample was calculated using the *gsva* method of the *Gsva* package. Patients were classified between high and low expression based on the median, and survival analysis was performed using the package *survival*. This analysis was validated in a second data set from Bailey *et al*.<sup>47</sup>

### Statistical analysis

Statistical analysis was performed in Graphpad Prism V.9.3.1. Comparison of KPC3 Mock tumors with KPC3 CMAS KO tumors was done using two-tailed unpaired Student t-test unless stated otherwise in the legend. The bars in graphs represent the SD and statistical significance was determined by a value of <0.05 (\* $p \leq 0.05$ , \*\* $p \leq 0.01$ , \*\*\* $p \leq 0.001$ , \*\*\*\* $p \leq 0.0001$ ; ns, not significant).

## RESULTS

### Establishing the mouse model to study tumor sialylation in vivo

To evaluate the impact of tumor sialylation on various dynamics of PDAC in vivo, we employed murine KPC3 cells, which is a PDAC model induced by KRAS and P53 mutations.<sup>43–44</sup> The KPC3 model recapitulates human PDAC features as the tumors contain an abundance of

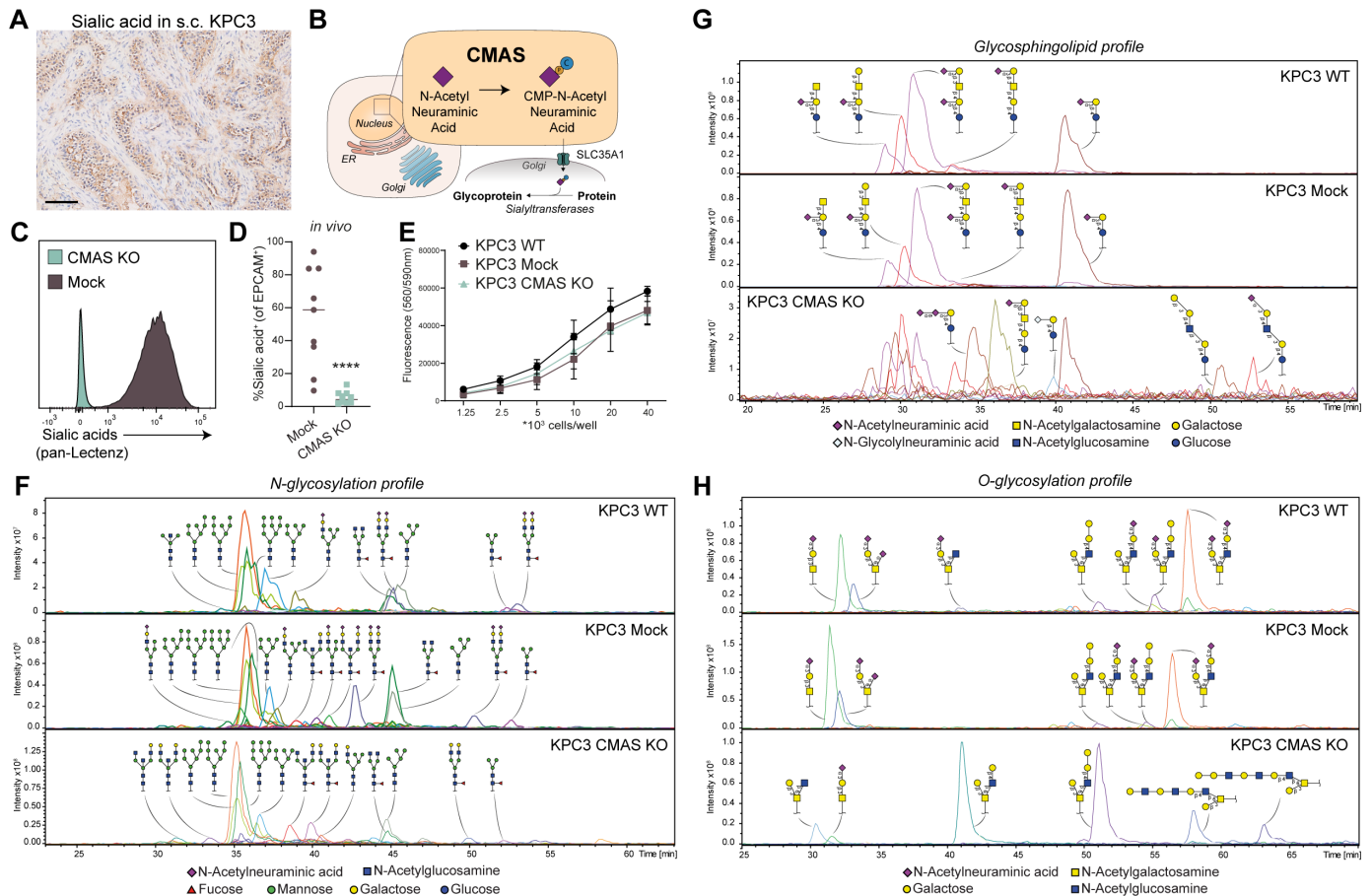


**Figure 1** CMAS KO in the KPC3 cells eliminates sialic acids from glycoproteins. (A) Sialic acid staining using pan-Lectenz in s.c. KPC3 WT tumor. Scale bar represents 100  $\mu$ m, representative image of  $n=5$ . (B) Schematic representation on the role of the CMAS enzyme in the sialylation pathway. (C) Sialic acid expression as evaluated by pan-Lectenz in KPC3 cell lines transfected with Mock construct (KPC3 Mock), or CRISPR/Cas9 construct for CMAS KO (KPC3 CMAS KO). (D) Sialic acid levels on EPCAM<sup>+</sup> tumor cells from s.c. KPC3 Mock and KPC3 CMAS KO tumors. Statistical analysis with Mann-Whitney test,  $n=9$  for KPC3 Mock and  $n=10$  for KPC3 CMAS KO. (E) Viability of KPC3 variants after 48 hours of culture as an indicator of proliferation of these cell lines. Data combined from three independent experiments. (F) *N*-glycan profiles of KPC3 variants determined by mass spectrometry. (G) Glycosphingolipid glycan profiles of KPC3 variants determined by mass spectrometry. (H) *O*-glycan profiles of KPC3 variants determined by mass spectrometry. Data presented as mean  $\pm$  SD. P value represented as \*\*\*\* $p \leq 0.0001$ . CMAS, cytidine monophosphate *N*-acetylneuraminic acid synthetase; KO, knock-out; s.c., subcutaneously; WT, wild-type.

stroma, and tumor islands expressed sialic acids as evaluated by immunohistochemistry using pan-Lectenz staining (figure 1A). To specifically investigate the influence of tumor sialylation, we generated a sialic acid-deficient variant of the KPC3 cells using CRISPR/Cas9 gene editing. This was achieved by knocking-out cytidine monophosphate *N*-acetylneuraminic acid synthetase (CMAS), an essential enzyme in the sialic acid metabolism pathway (figure 1B). Consequently, the CMAS KO resulted in removal of sialic acids on the membrane of the KPC3 cells both in vitro and in vivo (figure 1C,D). The absence of sialic acids on the cell surface did not impact proliferation of the KPC3 cells, nor did it affect major histocompatibility complex (MHC) class I expression (figure 1E, online supplemental figure S1A).

In order to validate the KO of sialic acid and to gain insight into the specific glycan structures expressed by the KPC3 cells, a comprehensive glycan profiling analysis was conducted, including the *O*-glycosylation, *N*-glycosylation

and glycosphingolipid glycosylation profiles. The KPC3 Mock transfected cells exhibited similar glycan profiles to the KPC3 WT cells, indicating that the transfection process did not alter the overall glycan profile of the cell lines (figure 1F–H, online supplemental figure S1B, online supplemental table 2). The analysis revealed that nearly all *O*-glycans and glycosphingolipid glycans were sialylated in the KPC3 WT and KPC3 Mock cells. The *N*-glycan profile showed that 20–30% of *N*-glycans were sialylated in KPC3 WT and Mock cells. Regarding the overall glycan profile of KPC3 WT and Mock cells, we observed that the cells expressed relatively high levels of sialyl-T (ST) and disialyl-T (di-ST) antigens (figure 1H), which are specific glycan structures often found on mucins. The presence of these glycans is associated with tumor progression and poor prognosis in several cancer types.<sup>48–51</sup>

In the context of the KPC3 CMAS KO cells, sialylation was significantly reduced or even absent, particularly on

*N*-glycans and *O*-glycans (figure 1F–H, online supplemental figure S1B). Surprisingly, the glycosphingolipid profile showed distinct features compared with the KPC3 WT and Mock, and although sialylation was reduced on glycosphingolipid glycans, the majority of glycosphingolipids remained sialylated in the KPC3 CMAS KO cells (figure 1G, online supplemental figure S1B). Additionally, the absence of sialic acid led to elongation of *O*-glycans, a pattern not observed for *N*-glycans (figure 1F,H).

Together, these data show that KO of CMAS in KPC3 cells results in a sustained lack of sialic acids on tumor cells in vitro and in vivo.

### Sialic acid-deficiency in KPC3 leads to a favorable T-cell landscape in the TME

To evaluate the effect of tumor sialylation on KPC3 tumor growth, mice were injected s.c. with the KPC3 cell lines. Loss of tumor sialylation was verified by immunohistochemistry (online supplemental figure S2A). Given the previously reported influence of sialic acid loss on tumor growth in other cancer types,<sup>29 34 39 40</sup> we hypothesized that sialic acid-deficiency would result in reduced KPC3 tumor growth as compared with sialic acid-expressing KPC3 tumors. Unexpectedly, the KPC3 CMAS KO cell line, that lack sialylated *N*-glycans and *O*-glycans, showed comparable tumor growth to the KPC3 Mock cells in vivo, indicating that tumor sialylation does not influence tumor growth (figure 2A,B, online supplemental figure S2B). Subsequently, we analyzed the cellular composition of the TME, including immune cells, CAFs, and endothelial cells. Interestingly, the KPC3 CMAS KO tumors demonstrated an increased proportion of immune cells, based on CD45 expression within in the TME (figure 2C). Notably, the sialylation KO had no effect on the relative abundance of endothelial cells (CD31<sup>+</sup>) and CAFs (PDPN<sup>+</sup>) within the tumor (figure 2C).

To gain further insight into the distinct immune cell subsets within these tumors, we employed a 24-color panel for spectral flow cytometry, enabling the identification of 19 distinct cell populations (figure 2D,E, online supplemental figure S2C). The majority of immune cells in KPC3 tumors belonged to the myeloid lineage, with the predominant cell type being neutrophils (figure 2D, online supplemental figure S2C,D). In contrast, lymphocytes were present in limited numbers, accounting for less than 10% of all immune cells (figure 2D, online supplemental figure S2D). Remarkably, the CD8<sup>+</sup> T-cell population was clustered in two subsets, distinguished by the expression of Ly6C (figure 2D,E, online supplemental figure S2C). While the precise functional distinctions conferred by Ly6C expression on CD8<sup>+</sup> T cells remain unclear, Ly6C-positive cells are associated with T-cell homing and have been linked to central memory and effector T-cell subsets.<sup>52–54</sup> To determine which cell clusters exhibited significant differences between KPC3 Mock and CMAS KO, we manually gated the identified populations (online supplemental figure

S3). Interestingly, the 3 T-cell subsets, CD8<sup>+</sup> T, CD8<sup>+</sup> Ly6C<sup>+</sup> T and CD4<sup>+</sup> T cells, showed a significant increase in KPC3 CMAS KO tumors compared with KPC3 Mock tumors (figure 2F). Next, we examined the immunosuppressive cell populations, specifically TAMs and Tregs. Surprisingly, we did not observe significant differences in TAM frequencies or MHC class II expression on TAMs (online supplemental figure S2E). However, a notable decrease in Tregs (CD4<sup>+</sup> Foxp3<sup>+</sup> T cells) was observed in the sialic acid-deficient tumors when analyzed within the T-cell population, indicating a shift in the CD8<sup>+</sup> T cell/Treg balance in the KPC3 CMAS KO tumors (figure 2G,H).

Collectively, these data demonstrate that tumor sialylation does not impact tumor growth, but exerts profound effects on the lymphoid immune landscape within the TME leading to a favorable T-cell profile.

Given the prevalence of T-cell exclusion in PDAC, we aimed to investigate the spatial distribution of the increased number of CD8<sup>+</sup> T cells within the tumor. To accomplish this, we performed immunofluorescent staining on KPC3 Mock and KPC3 CMAS KO tumors. Interestingly, CD8<sup>+</sup> T cells in the KPC3 CMAS KO tumors were localized in close proximity to the tumor islands in comparison to KPC3 Mock tumors (figure 2I). These findings provide evidence that absence of tumor sialylation can have the potential to reverse the immune-excluded phenotype found in PDAC.

### Tumor sialylation modulates the draining lymph node

Tumor cells can secrete sialylated carbohydrate antigens, such as the CA19-9 antigen (also known as sialyl Lewis A), which serves as a well-known biomarker for pancreatic cancer.<sup>55</sup> These sialylated antigens have the potential to drain to the lymph node and modulate immune function. Previous research has demonstrated that a reduction in tumor sialylation in melanoma can alter immune cell frequencies in the draining lymph node.<sup>29</sup> Therefore, we investigated the possible contribution of KPC3-derived sialic acids to immune suppression beyond the local tumor site, by examining immune subsets and co-stimulatory markers in both the tumor draining and non-draining lymph nodes (figure 3A,B, online supplemental figure S4A,B). The non-draining lymph nodes did not exhibit any differences in cell populations or activation states between KPC3 Mock and CMAS KO bearing mice (figure 3A–E, online supplemental figure S4C). However, within the tumor-draining lymph node, we observed an increase in B cells in the KPC3 CMAS KO tumor-bearing mice compared with KPC3 Mock tumor-bearing mice, implying an enhanced B-cell response (figure 3C). Furthermore, while the decrease in T-cell percentages did not reach statistical significance, it suggests a possible migration of T cells from the lymph node to the tumor site (figure 3D). Moreover, a reduction in CD4<sup>+</sup> CD25<sup>+</sup> T cells, potentially corresponding to Tregs, was observed, indicating a

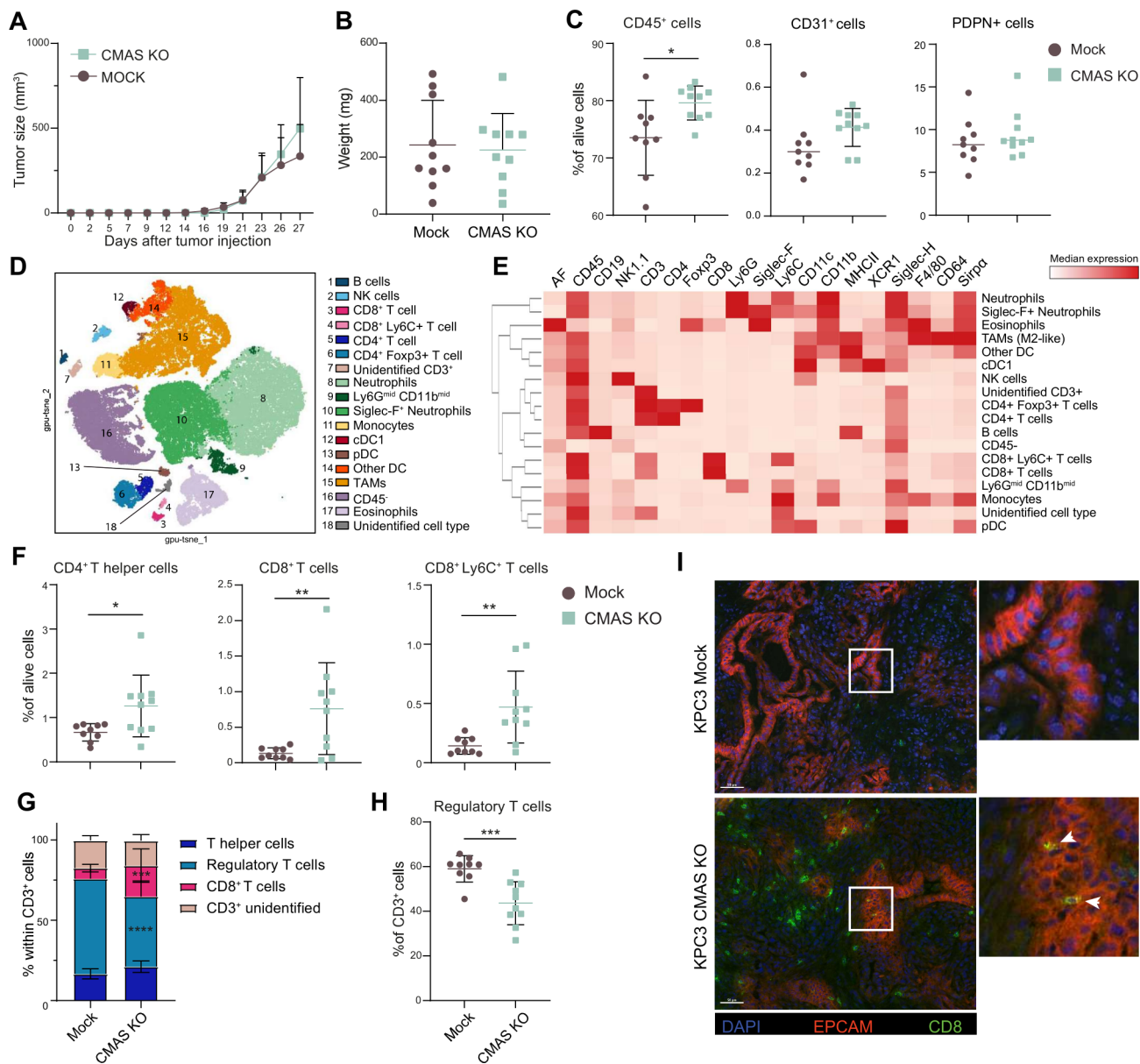


**Figure 2** Ablation of tumor sialylation alters the immune composition of the TME in murine PDAC. (A) Tumor size over time of s.c. injected KPC3 Mock and CMAS KO tumors. (B) KPC3 tumor weight at day 27 after injection. (C) Percentage of CD45<sup>+</sup> immune cells, CD31<sup>+</sup> endothelial cells and PDPN<sup>+</sup> CAFs in KPC3 Mock and CMAS KO tumors of A–B analyzed by spectral flow cytometry. (D) tSNE of unsupervised clustering analysis, showing the dimensional reduction and clustering of spectral flow cytometry data on alive cells in KPC3 tumors. (E) Heatmap of cell marker expression across cell clusters shown in D. (F) Percentage of different immune cell types in the different KPC3 tumors gated over alive cells. (G) Relative cell frequencies within the total CD3<sup>+</sup> T cells. Statistical analysis performed using two-way ANOVA with Bonferroni multiple comparison test comparing Mock and CMAS within the cell subsets. (H) Percentage of Treg cells over total CD3<sup>+</sup> T cells. (I) Representative image of immunofluorescence staining of EPCAM (red) and CD8 (green) in KPC3 tumors. Cell nuclei are stained with DAPI (blue). Data presented as mean±SD. For KPC3 Mock n=9 and for KPC3 CMAS KO n=10. P value represented as \*p≤0.05, \*\*p≤0.01, \*\*\*p≤0.001, \*\*\*\*p≤0.0001. ANOVA, analysis of variance; CAFs, cancer-associated fibroblasts; cDCs, classical DCs; CMAS, cytidine monophosphate N-acetylneuraminic acid synthetase; DCs, dendritic cells; KO, knock-out; NK, natural killer; PDAC, pancreatic ductal adenocarcinoma; pDCs, plasmacytoid DCs; s.c., subcutaneously; TAMs, tumor-associated macrophages; TME, tumor microenvironment; Tregs, regulatory T cells; t-SNE, t-Distributed Stochastic Neighbor Embedding.

diminished suppressive immune response within the draining lymph node of KPC3 CMAS KO bearing mice (figure 3D). Analysis of the antigen-presenting cells revealed higher expression levels of the co-stimulatory molecule CD80 and the inhibitory molecule programmed death-ligand 1 (PD-L1) in KPC3 CMAS

KO bearing mice, specifically in the CD11b<sup>mid</sup>Sirpa<sup>+</sup> subset (figure 3E). Percentages of other antigen presenting cell subsets were not affected by the CMAS KO (online supplemental figure S4C). Taken together, these results indicate that the absence of tumor-derived sialic acids selectively affects immune

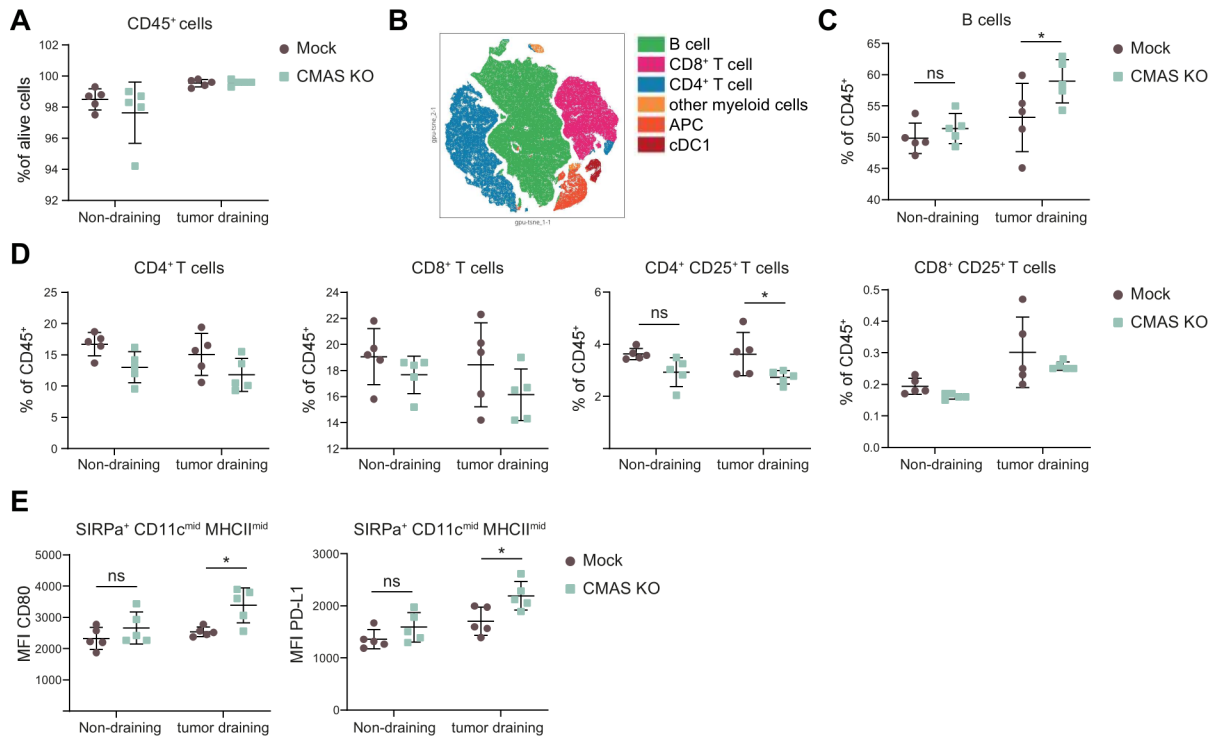


**Figure 3** Tumor sialylation alters immune cell populations in tumor-draining lymph nodes. (A) Percentage of CD45<sup>+</sup> immune cells in draining and non-draining lymph nodes of KPC3 tumor-bearing mice. (B) Dimensional reduction of CD45<sup>+</sup> immune cells in the lymph node based on spectral flow cytometry data. (C) Percentage B cells in the lymph nodes of KPC3 tumor-bearing mice. (D) Percentage of lymphoid subsets cells in the lymph nodes of KPC3 tumor-bearing mice. (E) Expression of CD80 and PD-L1 on antigen-presenting cell subsets in lymph nodes of KPC3 tumor-bearing mice. Data presented as mean±SD. Statistical analysis in C–E was done using two-way ANOVA with Bonferroni multiple comparison test comparing Mock and CMAS within the draining and non-draining lymph nodes. P value represented as \*p≤0.05, \*\*p≤0.01, \*\*\*p≤0.001, \*\*\*\*p≤0.0001. Total n=10 per group, lymph nodes of two mice were pooled after harvesting. ANOVA, analysis of variance; APC, antigen-presenting cell, cDCs, classical dendritic cells; CMAS, cytidine monophosphate N-acetylneuraminic acid synthetase; KO, knock-out; MFI, mean fluorescent intensity; MHC, major histocompatibility complex; PD-L1, programmed death-ligand 1.

responses within the draining lymph node, suggesting a localized rather than systemic impact on immune regulation by tumor-derived sialic acids.

### Sialic acid-deficiency synergizes with immunotherapy

Sialic acid deficient tumors showed a favorable T-cell landscape characterized by enhanced CD8<sup>+</sup> T cells and decreased Tregs. Despite this, their tumor growth remained comparable to sialic acid-expressing tumors, suggesting the presence of additional local immune cell constraints within the TME. Consequently, we hypothesized that immunotherapy could potentially augment T-cell activity in the KPC3 CMAS KO tumor, resulting in reduced tumor growth. Supporting this hypothesis, we observed the expression of PD-1 on both CD8<sup>+</sup> and CD4<sup>+</sup> T cells, with elevated expression on CD4<sup>+</sup> T cells in the KPC3 CMAS KO tumors (figure 4A). Given the ineffectiveness of ICB alone in PDAC, and the key role of myeloid cells in immune suppression, we aimed to target both T cells and myeloid cells using combination treatment of anti-PD-1 and agonistic CD40 antibodies.<sup>56,57</sup> Remarkably, the application of immunotherapy effectively reduced tumor growth and significantly improved the survival in the KPC3 CMAS KO bearing mice, while no discernible effect was observed in KPC3 Mock tumors (figure 4B,C).

These findings illustrate that the lack of sialic acids synergizes with immunotherapy in murine PDAC, overcoming the intrinsic resistance of PDAC to ICB.

### High expression of sialylation genes correlates with decreased CD8<sup>+</sup> T cells and increased Treg cell numbers in human PDAC

In order to extend the relevance of our findings from murine PDAC to human PDAC, we analyzed the expression of sialylation-related genes and their correlation with immune cell abundance and survival probability. Specifically we examined the genes involved in the donor synthesis pathway of sialylation. This pathway is critical for the biosynthesis of sialic acid precursors which can be attached to glycoproteins and glycolipids, and showed to be highly expressed in tumor cells (figure 5A), thus serving as a potential surrogate marker for tumor sialylation. Interestingly, the expression of donor synthesis genes showed the most significant correlation with CD8<sup>+</sup> T-cell abundance, with high expression of donor genes associated with low amounts of CD8<sup>+</sup> T cells (figure 5B, online supplemental figure S5A). In addition, patients with enriched expression of donor synthesis genes showed worse overall survival probability and disease-free survival probability (figure 5C, online supplemental figure S5B).

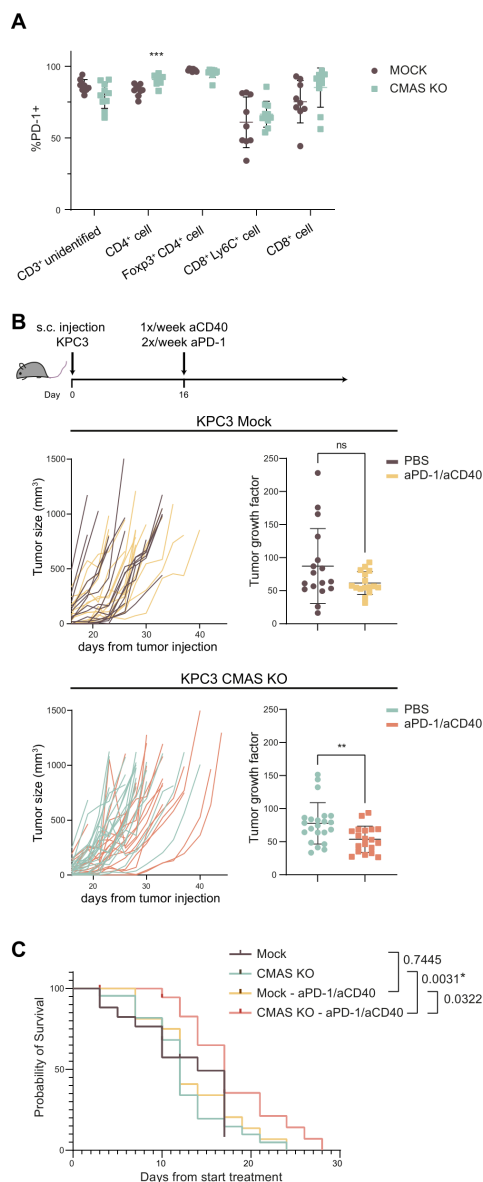


**Figure 4** Sialic acid-deficiency synergizes with immunotherapy. (A) Percentage of PD-1 expressing cells within lymphoid populations in KPC3 tumors. Data presented as mean $\pm$ SD. For KPC3 Mock n=9 and for KPC3 CMAS KO n=10. P value represented as \*\*\*p $\leq$ 0.001. (B) Individual tumor growth curves and tumor growth factor per mouse, treated or not with anti-PD-1 and agonistic CD40 antibodies (aPD-1/aCD40). KPC3 Mock or KPC3 CMAS KO tumors were established and treated at day 16. Tumor growth factor was calculated by fitting a linear curve ( $y=\alpha x+\beta$ ) to the tumor growth measurements from day 16 until the day of sacrifice, and plotting the  $\alpha$  (ie, average growth per day). Data presented as mean $\pm$ SD, with n=16–22 per group (Mock n=17, Mock - aPD-1/aCD40 n=16, CMAS KO n=22, CMAS KO - aPD-1/aCD40 n=19), and statistical analysis was performed with Mann-Whitney test. P value represented as \*\*p $\leq$ 0.01. (C) Survival curves of the mice from B. Statistical analysis was performed with log-rank (Mantel-Cox) test. Statistical significance was reached when p $\leq$ 0.0167 (Bonferroni corrected) as marked by \*. CMAS, cytidine monophosphate N-acetylneuraminic acid synthetase; KO, knock-out; PBS, phosphate-buffered saline; PD-1, programmed cell death protein 1.

Among the analyzed genes, *CMAS* exhibited the most pronounced expression in tumor cells compared with other cell types (figure 5D). Importantly, *CMAS* expression showed a significant positive correlation with the abundance of Tregs (figure 5E, online supplemental figure S5C). This observation suggests that elevated tumor sialylation in human PDAC may be associated not only with reduced CD8<sup>+</sup> T-cell infiltration but also with an increased number of Tregs. Collectively, these findings show the potential impact of tumor sialylation on survival probability, lymphocyte abundance and immune regulation in the context of human PDAC.

## DISCUSSION

The application of immunotherapy in PDAC has encountered substantial challenges due to the immunosuppressive TME, limited tumor immunogenicity, and the development of resistance mechanisms that hinder the efficacy of immune checkpoint inhibitors. CD8<sup>+</sup> T-cell infiltration, which is crucial for the effectiveness of ICB, is typically limited in PDAC tumors. In this study, we aimed to investigate the role of tumor sialylation, a novel potential target for immunotherapy, in tumor growth and modulation of the immune TME. Our data demonstrates that sialic acid deficiency can convert the TME to a state that allows for enhanced numbers of CD8<sup>+</sup> T cells infiltrating the tumor. Consequently, by reversing the immune excluded phenotype, we observed a significant improvement in the survival of tumor-bearing mice on treatment with immunotherapy.

Previous preclinical studies in other cancer types consistently demonstrated that reducing sialic acid expression on tumor cells decreased tumor growth and improved survival.<sup>29 34 39 40</sup> In contrast to these reports, our findings revealed that loss of sialic acids by itself did not affect tumor growth in murine PDAC (figure 2A,B). This discrepancy can be attributed to several factors specific to PDAC. First, PDAC exhibits low levels of tumor antigens as compared with other tumor types, limiting the recognition of tumor cells by the immune system.<sup>3</sup> Second, the immunosuppressive environment creates formidable barriers to reduce tumor growth through immune modulation.<sup>4</sup> Moreover, a notable distinction between PDAC and other tumor types is the presence of dense fibrotic stroma, which profoundly shapes the TME and contributes to disease aggressiveness.<sup>4</sup> Targeting both the tumor and stroma may be necessary for therapeutic success in PDAC, and this concept can extend to the manipulation of sialic acids. Notably, stromal cells themselves have been reported to express sialic acids,<sup>58</sup> indicating that solely targeting tumor cell sialylation may not be sufficient to inhibit tumor growth in PDAC, necessitating the consideration of stromal sialylation as well.

Although the lack of tumor sialylation did not directly impact tumor growth, our study revealed significant alterations in local immune compositions within the TME and tumor-draining lymph nodes. In the TME, we observed

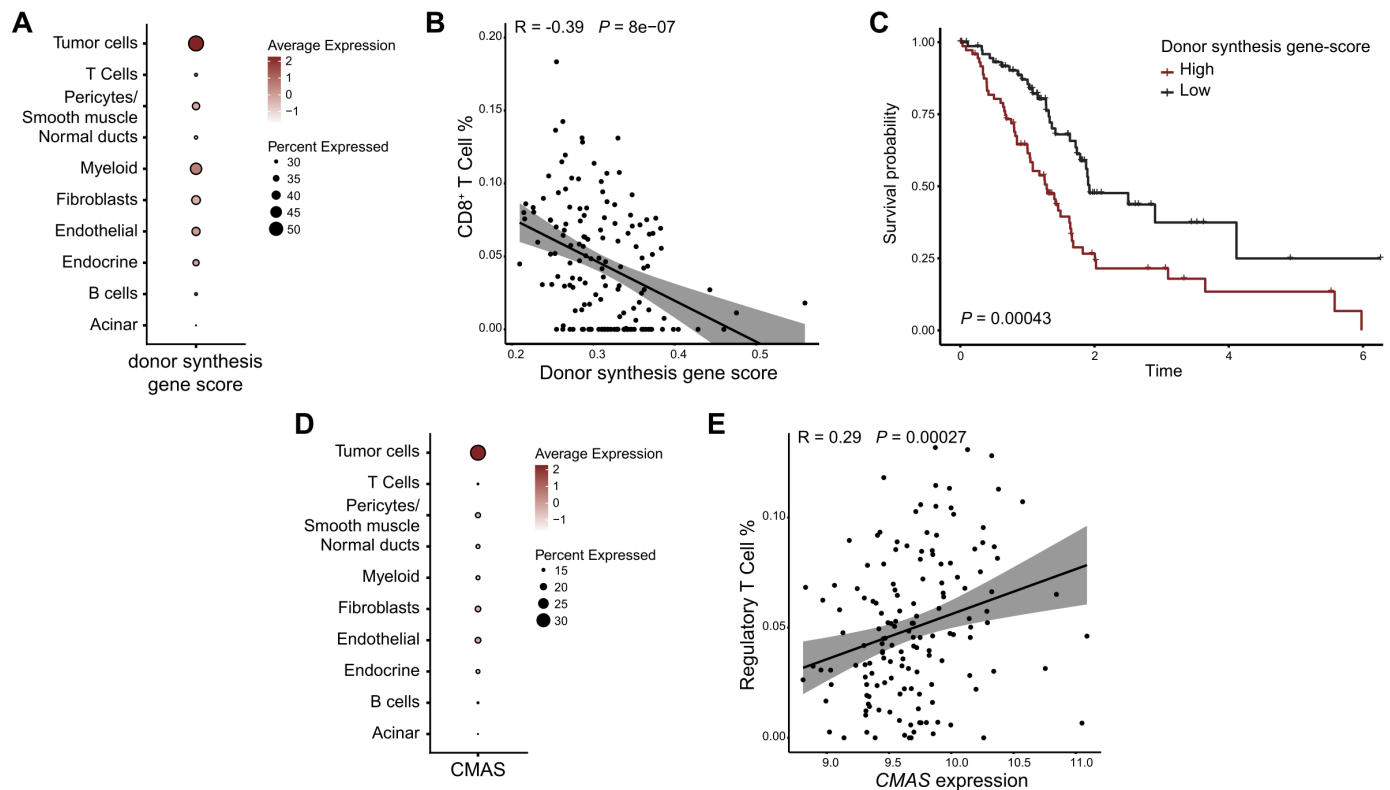


**Figure 5** Sialylation gene expression correlates with T-cell abundance in human PDAC. (A) Expression of donor synthesis genes, based on a gene score, in different cell subsets in PDAC, analyzed using the single-cell RNA sequencing data set of PDAC patients from Peng *et al.*<sup>45</sup> (B) Spearman correlation between donor synthesis gene score and CD8<sup>+</sup> T-cell abundance as identified by tumor microenvironment deconvolution (Cibersort) in human PDAC tumors, analyzed in bulk sequencing data (TCGA). (C) Kaplan-Meier curve showing the survival probability of patients with PDAC from TCGA data set, stratified by high versus low expression of donor synthesis genes. Statistical analysis performed using Cox Regression. (D) Expression of CMAS in different cell subsets in PDAC, analyzed using the single-cell RNA sequencing data set of patients with PDAC from Peng *et al.*<sup>45</sup> (E) Spearman correlation between the expression of CMAS enzyme and the estimated abundance of Treg cells as identified by tumor microenvironment deconvolution (Cibersort) in human PDAC tumors, analyzed in bulk sequencing data (TCGA). CMAS, cytidine monophosphate N-acetylneuraminic acid synthetase; PDAC, pancreatic ductal adenocarcinoma; TCGA, The Cancer Genome Atlas; Tregs, regulatory T cells.

an augmentation of tumor-infiltrating lymphocytes and a decrease in Tregs, indicating a potential shift towards an immune-inflamed state. Notably, classical DCs (cDC), which are essential for an effective antitumor T-cell response and immunotherapy response,<sup>59–60</sup> did not exhibit significant alterations in their subsets or co-stimulatory molecule expression in the draining lymph node. This suggests that the increased lymphocyte presence in the KPC3 CMAS KO tumors may involve mechanisms independent of priming by cDCs in the draining lymph node.

Sialic acids have been widely investigated for their involvement in driving macrophage polarization towards a tumor-promoting phenotype.<sup>34–38, 41, 42, 61</sup> However, in contrast to these findings, our study did not observe significant alterations in frequencies or MHC class II expression of TAMs in sialic acid-deficient tumors. This finding was unexpected, considering that KPC3 cells express sialylated glycans such as the ST-antigen (figure 1H), which has been reported to influence myeloid differentiation to a TAM phenotype in the context of breast cancer.<sup>36</sup> Furthermore, the sialylated glycans on KPC3

resemble the glycan profile of human PDAC cell lines which also express ST and di-ST,<sup>17</sup> and we have previously demonstrated that PDAC cell lines modulate TAM differentiation through sialic acids *in vitro*.<sup>42</sup> Besides, the effects of sialic acids on tumor growth and immune modulation have been shown to be dependent on mouse Siglec-E, primarily expressed on myeloid cells.<sup>34</sup> Although T cells can express Siglec-E in certain settings,<sup>27, 28</sup> we did not observe its expression on T cells in our study (data not shown). Thus, while the frequencies of myeloid populations and MHC class II expression on TAMs remained unchanged, it is plausible that functional alterations in myeloid cells, potentially mediated through sialic acid-Siglec interactions, contributed to the establishment of a more inflamed TME that influenced T-cell infiltration.

Interestingly, sialic acid-deficiency made our KPC3 tumor responsive to immunotherapy (figure 4B). Surprisingly, the treatment with anti-PD-1 and agonistic CD40 antibodies was shown to be ineffective in the KPC3 Mock tumors, despite its reported therapeutic efficacy in other PDAC studies.<sup>57, 62, 63</sup> The lack of response to immunotherapy is often associated with the limited neo-antigen

expression in PDAC or inadequate immune cell infiltration.<sup>3</sup> The inadequate immune cell infiltration, particularly of CD8<sup>+</sup> T cells, was reversed by the absence of tumor sialylation in the KPC3 CMAS KO, which could underlie the responsiveness to immunotherapy in these tumors. Nevertheless, although immunotherapy significantly improved survival and delayed tumor growth in the KPC3 CMAS KO tumor-bearing mice, the magnitude of this effect remained small and no mice were cured. Combining immunotherapy with sialic acid removal in a setting with sufficient tumor-antigen specific T cells, for example, by vaccination strategies, may further enhance the therapeutic efficacy.

The amount of T cells and their proximity to tumor cells is known to be associated with better survival outcomes in patients with PDAC.<sup>9 14–16</sup> Consequently, targeting sialic acids in patients with PDAC offers the potential to augment T cell numbers and overcome the immune excluded phenotype of the TME. In recent years, several strategies have emerged for targeting sialic acids, including tumor-targeted degradation of sialic acids and sialic acid mimetics that inhibit sialyltransferase activity.<sup>39 40 64</sup> A phase I clinical trial, which includes patients with PDAC, is currently investigating the safety and potential of sialidase treatment (NCT05259696). Initial results of this trial with systemic administration of the bi-sialidases show that the compound was well tolerated with no dose limiting toxicities. These therapeutic approaches represent promising avenues for combination therapy in PDAC, particularly when combined with agents that enhance T-cell function.

In this study we use a complete and durable KO of sialic acids to study the role of sialic acids in PDAC. However, in patients, we observed heterogeneity in donor synthesis gene expression including *CMAS*, and interestingly, we found a correlation between these gene levels and the abundance of CD8<sup>+</sup> T cells and Tregs. This suggests that *CMAS* expression levels could potentially serve as a biomarker for a favorable T-cell landscape. Taking into account the absolute deficiency of sialic acids compared with the varying levels in humans, it is crucial to consider the consequences of sialylation loss on underlying glycan structures. This loss exposes terminal galactose residues (figure 1H), which can serve as binding sites for galectins, introducing an additional layer of complexity. For instance, it has been described that silencing of *ST6GALNAC2* decreases di-ST expression and creates binding sites for galectin-3, which in turn leads to increased metastatic burden in breast cancer.<sup>65</sup> Modulating sialylation levels in patients to decrease their sialic acid expression may offer a more favorable approach compared with the complete removal of sialic acids. Next to potential binding of galectins, loss of tumor sialylation may also affect tumor cell survival, invasion or metastasis.<sup>66</sup>

In conclusion, our study demonstrates that the absence of sialic acids, achieved through genetic depletion of *CMAS*, leads to favorable alterations in the immune landscape of pancreatic tumors and the draining lymph

node. Specifically, we observed increased frequencies of CD4<sup>+</sup> helper and CD8<sup>+</sup> cytotoxic T cells, accompanied by a reduction in Tregs within the T-cell population in the TME. Notably, mice with sialic acid-deficient tumors showed improved survival in response to immunotherapy, while those with sialylated tumors did not exhibit survival benefits. Importantly, our findings extend to the clinical context, as higher expression of sialylation genes in human pancreatic cancer is associated with decreased CD8<sup>+</sup> T-cell infiltration and increased Treg presence, and worse patient outcome. These results highlight the critical role of tumor sialylation in shaping the tumor immune microenvironment and provide insights for the development of targeted immunotherapeutic strategies in pancreatic cancer.

**Acknowledgements** We acknowledge the Microscopy and Cytometry Core Facility at the Amsterdam UMC – Location VUmc for providing assistance in our microscopy and cytometry work. In particular, we would like to acknowledge Liesbeth Paul for the design and advice on Spectral flow cytometry panels.

**Contributors** KB and YVK conceived the study. KB, LK, DW, CMdW, lvdHA, AdH, LB, REM, NvM, MW, SVV, YVK designed experiments or provided essential technical support. KB, LK, BS, LW acquired experimental data. KB, CMdW, BS analyzed data. DW, MW performed glycan profiling. KB, DL, ER performed transcriptomic analysis. KB and YVK drafted the manuscript. KB, LK, DW, CMdW, DL, ER, BS, lvdHA, AdH, LB, REM, NvM, MW, JMMDH, SVV, YVK provided critical intellectual content. YVK supervised the study and is responsible for the overall content as guarantor.

**Funding** This work is financially supported by KWF VU2014-7200 to KB; SPINOZANWO SPI-93-538 to KB, LK, LW and YVK; LSH-TKI project DC4Balance LSM1806-SGFLSH-TKI to AdH; CMdW is supported by Cancer Center Amsterdam (grant no. CCA2019-9-57 and CCA2020-9-73).

**Competing interests** None declared.

**Patient consent for publication** Not applicable.

**Ethics approval** All animal experiments were approved by the Animal Experiments Committee of the VU University (DEC201512, protocols 1024-MCB20-45; 1024-MCB20-58; 1024-MCB20-59; 1024-MCB21-66; 1024-MCB21-67) and performed in accordance with national and international guidelines and regulations

**Provenance and peer review** Not commissioned; externally peer reviewed.

**Data availability statement** Data are available upon reasonable request.

**Supplemental material** This content has been supplied by the author(s). It has not been vetted by BMJ Publishing Group Limited (BMJ) and may not have been peer-reviewed. Any opinions or recommendations discussed are solely those of the author(s) and are not endorsed by BMJ. BMJ disclaims all liability and responsibility arising from any reliance placed on the content. Where the content includes any translated material, BMJ does not warrant the accuracy and reliability of the translations (including but not limited to local regulations, clinical guidelines, terminology, drug names and drug dosages), and is not responsible for any error and/or omissions arising from translation and adaptation or otherwise.

**Open access** This is an open access article distributed in accordance with the Creative Commons Attribution Non Commercial (CC BY-NC 4.0) license, which permits others to distribute, remix, adapt, build upon this work non-commercially, and license their derivative works on different terms, provided the original work is properly cited, appropriate credit is given, any changes made indicated, and the use is non-commercial. See <http://creativecommons.org/licenses/by-nc/4.0/>.

#### ORCID iDs

Kelly Boelaars <http://orcid.org/0000-0002-2826-3027>

Ernesto Rodriguez <http://orcid.org/0000-0002-3855-5664>

Nadine van Montfoort <http://orcid.org/0000-0002-7906-7202>

Yvette van Kooyk <http://orcid.org/0000-0001-5997-3665>

## REFERENCES

- 1 Siegel RL, Miller KD, Wagle NS, et al. Cancer statistics, 2023. *CA Cancer J Clin* 2023;73:17–48.
- 2 Hosein AN, Dougan SK, Aguirre AJ, et al. Translational advances in Pancreatic Ductal adenocarcinoma therapy. *Nat Cancer* 2022;3:272–86.
- 3 Hegde PS, Chen DS. Top 10 challenges in cancer Immunotherapy. *Immunity* 2020;52:17–35.
- 4 Ho WJ, Jaffee EM, Zheng L. The tumour Microenvironment in Pancreatic cancer - clinical challenges and opportunities. *Nat Rev Clin Oncol* 2020;17:527–40.
- 5 Cassetta L, Pollard JW. A Timeline of tumour-associated macrophage biology. *Nat Rev Cancer* 2023;23:238–57.
- 6 Vignali DAA, Collison LW, Workman CJ. How regulatory T cells work. *Nat Rev Immunol* 2008;8:523–32.
- 7 Väyrynen SA, Zhang J, Yuan C, et al. Composition, spatial characteristics and Prognostic significance of myeloid cell infiltration in Pancreatic cancer. *Clin Cancer Res* 2021;27:1069–81.
- 8 Liudahl SM, Betts CB, Sivagnanam S, et al. Leukocyte heterogeneity in Pancreatic Ductal adenocarcinoma: Phenotypic and spatial features associated with clinical outcome. *Cancer Discov* 2021;11:2014–31.
- 9 Kiryu S, Ito Z, Suka M, et al. Prognostic value of immune factors in the tumor Microenvironment of patients with Pancreatic Ductal adenocarcinoma. *BMC Cancer* 2021;21:1197.
- 10 Wartenberg M, Cibin S, Zlobec I, et al. Integrated Genomic and Immunophenotypic classification of Pancreatic cancer reveals three distinct subtypes with Prognostic/predictive significance. *Clin Cancer Res* 2018;24:4444–54.
- 11 Provenzano PP, Cuevas C, Chang AE, et al. Enzymatic targeting of the Stroma Ablates physical barriers to treatment of Pancreatic Ductal adenocarcinoma. *Cancer Cell* 2012;21:418–29.
- 12 Beatty GL, Winograd R, Evans RA, et al. Exclusion of T cells from Pancreatic Carcinomas in mice is regulated by Ly6C(Low) F4/80(+) Extratumoral Macrophages. *Gastroenterology* 2015;149:201–10.
- 13 Hartmann N, Giese NA, Giese T, et al. Prevailing role of contact guidance in Intrastromal T-cell trapping in human Pancreatic cancer. *Clin Cancer Res* 2014;20:3422–33.
- 14 Masugi Y, Abe T, Ueno A, et al. Characterization of spatial distribution of tumor-infiltrating Cd8(+) T cells refines their Prognostic utility for Pancreatic cancer survival. *Mod Pathol* 2019;32:1495–507.
- 15 Carstens JL, Correa de Sampaio P, Yang D, et al. Spatial computation of Intratumoral T cells correlates with survival of patients with Pancreatic cancer. *Nat Commun* 2017;8:15095.
- 16 Ino Y, Yamazaki-Itoh R, Shimada K, et al. Immune cell infiltration as an indicator of the immune Microenvironment of Pancreatic cancer. *Br J Cancer* 2013;108:914–23.
- 17 Rodriguez E, Boelaars K, Brown K, et al. Analysis of the Glyco-code in Pancreatic Ductal adenocarcinoma identifies Glycan-mediated immune regulatory circuits. *Commun Biol* 2022;5:41.
- 18 Pinho SS, Reis CA. Glycosylation in cancer: mechanisms and clinical implications. *Nat Rev Cancer* 2015;15:540–55.
- 19 Bellis SL, Reis CA, Varki A, et al. Glycosylation changes in cancer. In: th, Varki A, Cummings RD, Esko JD, et al., eds. *Essentials of Glycobiology*. NY: Cold Spring Harbor, 2022: 631–44.
- 20 Rodríguez E, Schettters STT, van Kooyk Y. The tumour Glyco-code as a novel immune Checkpoint for Immunotherapy. *Nat Rev Immunol* 2018;18:204–11.
- 21 Lewis AL, Chen X, Schnaar RL, et al. Sialic acids and other Nonulosonic acids. In: th VA, RD C, JD E, et al., eds. *Essentials of Glycobiology*. NY: Cold Spring Harbor, 2022: 185–204.
- 22 Lübbers J, Rodríguez E, van Kooyk Y. Modulation of immune tolerance via Siglec-Sialic acid interactions. *Front Immunol* 2018;9:2807.
- 23 Angata T, Gunten S, Schnaar RL, et al. I-type Lectins. In: th, Varki A, Cummings RD, Esko JD, et al., eds. *Essentials of Glycobiology*. NY: Cold Spring Harbor, 2022: 475–90.
- 24 Jandus C, Boligan KF, Chijioke O, et al. Interactions between Siglec-7/9 receptors and ligands influence NK cell-dependent tumor Immunoreveillance. *J Clin Invest* 2014;124:1810–20.
- 25 Hudak JE, Canham SM, Bertozzi CR. Glycocalyx engineering reveals a Siglec-based mechanism for NK cell Immunoevasion. *Nat Chem Biol* 2014;10:69–75.
- 26 Daly J, Sarkar S, Natoni A, et al. Targeting Hypersialylation in multiple myeloma represents a novel approach to enhance NK cell-mediated tumor responses. *Blood Adv* 2022;6:3352–66.
- 27 Stanczak MA, Siddiqui SS, Trefny MP, et al. Self-associated molecular patterns mediate cancer immune evasion by engaging Siglecs on T cells. *J Clin Invest* 2018;128:4912–23.
- 28 Haas Q, Boligan KF, Jandus C, et al. Siglec-9 regulates an Effector memory Cd8(+) T-cell subset that Congregates in the Melanoma tumor Microenvironment. *Cancer Immunol Res* 2019;7:707–18.
- 29 Perdicchio M, Cornelissen LAM, Streng-Ouwehand I, et al. Tumor Sialylation Impedes T cell mediated anti-tumor responses while promoting tumor associated-regulatory T cells. *Oncotarget* 2016;7:8771–82.
- 30 Xiao H, Woods EC, Vukojicic P, et al. Precision Glycocalyx editing as a strategy for cancer Immunotherapy. *Proc Natl Acad Sci U S A* 2016;113:10304–9.
- 31 Wang J, Manni M, Bärenwaldt A, et al. Siglec receptors modulate Dendritic cell activation and antigen presentation to T cells in cancer. *Front Cell Dev Biol* 2022;10.
- 32 Perdicchio M, Ilarregui JM, Verstege MI, et al. Sialic acid-modified antigens impose tolerance via inhibition of T-cell proliferation and de novo induction of regulatory T cells. *Proc Natl Acad Sci U S A* 2016;113:3329–34.
- 33 Ding Y, Guo Z, Liu Y, et al. The lectin Siglec-G inhibits Dendritic cell cross-presentation by impairing MHC class I-peptide complex formation. *Nat Immunol* 2016;17:1167–75.
- 34 Stanczak MA, Rodrigues Mantuano N, Kirchhammer N, et al. Targeting cancer Glycosylation Repolarizes tumor-associated Macrophages allowing effective immune Checkpoint blockade. *Sci Transl Med* 2022;14:eabj1270.
- 35 Friedman DJ, Crofts SB, Shapiro MJ, et al. St8Sia6 promotes tumor growth in mice by inhibiting immune responses. *Cancer Immunol Res* 2021;9:952–66.
- 36 Beatson R, Tajadura-Ortega V, Achkova D, et al. The Mucin Muc1 modulates the tumor immunological Microenvironment through engagement of the lectin Siglec-9. *Nat Immunol* 2016;17:1273–81.
- 37 Wang J, Sun J, Liu LN, et al. Siglec-15 as an immune Suppressor and potential target for normalization cancer Immunotherapy. *Nat Med* 2019;25:656–66.
- 38 Barkal AA, Brewer RE, Markovic M, et al. Cd24 signalling through macrophage Siglec-10 is a target for cancer Immunotherapy. *Nature* 2019;572:392–6.
- 39 Büll C, Boltje TJ, Balneger N, et al. Sialic acid blockade suppresses tumor growth by enhancing T-cell-mediated tumor immunity. *Cancer Res* 2018;78:3574–88.
- 40 Gray MA, Stanczak MA, Mantuano NR, et al. Targeted Glycan degradation potentiates the anticancer immune response in vivo. *Nat Chem Biol* 2020;16:1376–84.
- 41 Ibarlucea-Benitez I, Weitzenfeld P, Smith P, et al. Siglecs-7/9 function as inhibitory immune checkpoints in vivo and can be targeted to enhance therapeutic antitumor immunity. *Proc Natl Acad Sci USA* 2021;118:26.
- 42 Rodriguez E, Boelaars K, Brown K, et al. Sialic acids in Pancreatic cancer cells drive tumour-associated macrophage differentiation via the Siglec receptors Siglec-7 and Siglec-9. *Nat Commun* 2021;12.
- 43 Lee JW, Komar CA, Bengsch F, et al. Genetically engineered Mouse models of Pancreatic cancer: the KPC model (LSL-Kras(G12D/+);LSL-Trp53(R172H/+);Pdx-1-CRE), its variants, and their application in Immuno-oncology drug discovery. *Curr Protoc Pharmacol* 2016;73:14.
- 44 Groeneveldt C, Kinderman P, van den Wollenberg DJM, et al. Preconditioning of the tumor Microenvironment with Oncolytic Reovirus converts Cd3-Bispecific antibody treatment into effective Immunotherapy. *J Immunother Cancer* 2020;8:e001191.
- 45 Peng J, Sun B-F, Chen C-Y, et al. Single-cell RNA-Seq highlights intra-Tumoral heterogeneity and malignant progression in Pancreatic Ductal adenocarcinoma. *Cell Res* 2019;29:725–38.
- 46 Peran I, Madhavan S, Byers SW, et al. Curation of the Pancreatic Ductal adenocarcinoma subset of the cancer genome Atlas is essential for accurate conclusions about survival-related molecular mechanisms. *Clin Cancer Res* 2018;24:3813–9.
- 47 Bailey P, Chang DK, Nones K, et al. Genomic analyses identify molecular subtypes of Pancreatic cancer. *Nature* 2016;531:47–52.
- 48 Arai T, Fujita K, Fujime M, et al. Expression of Sialylated Muc1 in prostate cancer: relationship to clinical stage and prognosis. *Int J Urol* 2005;12:654–61.
- 49 Kawamoto T, Shoda J, Miyahara N, et al. Expression of Muc1 recognized by Monoclonal antibody MY.1E12 is a useful biomarker for tumor aggressiveness of advanced colon carcinoma. *Clin Exp Metastasis* 2004;21:353–62.
- 50 Picco G, Julien S, Brockhausen I, et al. Over-expression of St3Gal-I promotes Mammary tumorigenesis. *Glycobiology* 2010;20:1241–50.
- 51 Bai R, Luan X, Zhang Y, et al. The expression and functional analysis of the Sialyl-T antigen in prostate cancer. *Glycoconj J* 2020;37:423–33.



- 52 Ju Y-J, Lee S-W, Kye Y-C, *et al.* Self-reactivity controls functional diversity of naive Cd8(+) T cells by Co-opting tonic type I interferon. *Nat Commun* 2021;12:6059.
- 53 Smith NL, Patel RK, Reynaldi A, *et al.* Developmental origin governs Cd8<sup>+</sup> T cell fate decisions during infection. *Cell* 2018;174:117–30.
- 54 Hänninen A, Maksimow M, Alam C, *et al.* Ly6C supports preferential homing of central memory Cd8<sup>+</sup> T cells into lymph nodes. *Eur J Immunol* 2011;41:634–44.
- 55 Poruk KE, Gay DZ, Brown K, *et al.* The clinical utility of CA 19-9 in Pancreatic adenocarcinoma: diagnostic and Prognostic updates. *Curr Mol Med* 2013;13:340–51.
- 56 Ullman NA, Burchard PR, Dunne RF, *et al.* Immunologic strategies in Pancreatic cancer: making cold tumors hot. *J Clin Oncol* 2022;40:2789–805.
- 57 Beatty GL, Chiorean EG, Fishman MP, *et al.* Cd40 agonists alter tumor Stroma and show efficacy against Pancreatic carcinoma in mice and humans. *Science* 2011;331:1612–6.
- 58 Egan H, Treacy O, Lynch K, *et al.* Targeting Stromal cell Sialylation reverses T cell-mediated immunosuppression in the tumor Microenvironment. *Cell Rep* 2023;42:112475.
- 59 Hegde S, Krisnawan VE, Herzog BH, *et al.* Dendritic cell paucity leads to dysfunctional immune surveillance in Pancreatic cancer. *Cancer Cell* 2020;37:289–307.
- 60 Binnewies M, Mujal AM, Pollack JL, *et al.* Unleashing Type-2 Dendritic cells to drive protective antitumor Cd4<sup>+</sup> T cell immunity. *Cell* 2019;177:556–71.
- 61 Beatson R, Graham R, Grundland Freile F, *et al.* Cancer-associated Hypersialylated Muc1 drives the differentiation of human monocytes into Macrophages with a pathogenic phenotype. *Commun Biol* 2020;3:644.
- 62 Vonderheide RH. Cd40 agonist antibodies in cancer Immunotherapy. *Annu Rev Med* 2020;71:47–58.
- 63 O'Hara MH, O'Reilly EM, Varadhachary G, *et al.* Cd40 agonistic Monoclonal antibody Apx005m (Sotigalimab) and chemotherapy, with or without Nivolumab, for the treatment of metastatic Pancreatic adenocarcinoma: an open-label, Multicentre, phase 1B study. *Lancet Oncol* 2021;22:118–31.
- 64 Läubli H, Nalle SC, Maslyar D. Targeting the Siglec-Sialic acid immune axis in cancer: current and future approaches. *Cancer Immunol Res* 2022;10:1423–32.
- 65 Murugaesu N, Iravani M, van Weverwijk A, *et al.* An in vivo functional screen identifies St6Galnac2 Sialyltransferase as a breast cancer metastasis Suppressor. *Cancer Discov* 2014;4:304–17.
- 66 Dobie C, Skropeta D. Insights into the role of Sialylation in cancer progression and metastasis. *Br J Cancer* 2021;124:76–90.